Cooper Pairing Above the Critical Temperature in a Unitary Fermi Gas

Gabriel Wlazłowski, Piotr Magierski, Joaquín E. Drut, Aurel Bulgac, and Kenneth J. Roche

Phys. Rev. Lett. **110**, 090401 — Published 26 February 2013

DOI: 10.1103/PhysRevLett.110.090401

NT@UW-12-17

Cooper pairing above the critical temperature in a unitary Fermi gas

Gabriel Wlazłowski[1,2], Piotr Magierski[1,2], Joaquín E. Drut[3], Aurel Bulgac[2] and Kenneth J. Roche[4,2]
[1] *Faculty of Physics, Warsaw University of Technology, Ulica Koszykowa 75, 00-662 Warsaw, POLAND*
[2] *Department of Physics, University of Washington, Seattle, Washington 98195–1560, USA*
[3] *Department of Physics and Astronomy, University of North Carolina, Chapel Hill, NC 27599-3255, USA* and
[4] *Pacific Northwest National Laboratory, Richland, WA 99352, USA*
(Dated: January 22, 2013)

We present an *ab initio* determination of the spin response of the unitary Fermi gas. Based on finite temperature quantum Monte Carlo calculations and the Kubo linear-response formalism, we determine the temperature dependence of the spin susceptibility and the spin conductivity. We show that both quantities exhibit suppression above the critical temperature of the superfluid-to-normal phase transition due to Cooper pairing. The spin diffusion transport coefficient does not display a minimum in the vicinity of the critical temperature and drops to very low values $D_s \approx 0.8\,\hbar/m$ in the superfluid phase. All these spin observables show a smooth and monotonic behavior with temperature when crossing the critical temperature T_c, until the Fermi liquid regime is attained at the temperature T^*, above which the pseudogap regime disappears.

PACS numbers: 03.75.Ss, 05.60.Gg, 51.20.+d, 05.30.Fk

There are basically two flavors of superfluids: fermionic and bosonic. The bosonic superfluid is realized when typically weakly interacting bosons condense and form a Bose-Einstein condensate (BEC). The typical fermionic superfluid is of Bardeen-Cooper-Schrieffer (BCS) type, where fermions in time-reversed orbitals form weakly-bound Cooper pairs and with increasing interaction strength turn into a BEC of Cooper pairs. The BEC superfluidity vanishes when the condensate fraction ceases to have a macroscopic value with increasing temperature and the long-range coherence is lost. On the other hand, when a BCS superfluid undergoes a phase transition to a normal state, Cooper pairs break due to thermal motion and there are no more bosonic constituents left to form a BEC. With the experimental confirmation of the BCS-BEC crossover in fermionic cold gases [1, 2], it became clear that one can have a new kind of system where both bosonic and fermionic superfluid features are present at the same time. The paradigmatic example is the unitary Fermi gas (UFG) where, unlike the BCS or BEC cases, the inter-particle interaction is strong, and the binding energy of the Cooper pair is comparable to the Fermi energy. It is believed that the unpolarized unitary Fermi gas, in a temperature region just above the critical temperature T_c, exists in a state which is neither fully bosonic nor fully fermionic in character, called the pseudogap state, widely studied in high-T_c superconductors (HTSC) [3, 4]. This is a temperature regime where a significant fraction of the Cooper pairs is present, even though the long-range coherence among them is lost, as is superfluidity. While the existence of the pseudogap regime in HTSC is an experimentally well known fact, the nature of the corresponding regime around the critical temperature T_c of the UFG has remained an open question. It is a tantalizing question, whether the pseudogap regime exists in dilute neutron matter as well. The properties of the neutron superfluid in the neutron star crust are very similar to those of the unitary gas, as highlighted by Bertsch's 1999 Many-Body X challenge. The reliable calculation of the neutrino processes in neutron stars, controlled by the neutron spin response [5], is a long standing problem and the present results will likely shed new light on these phenomena.

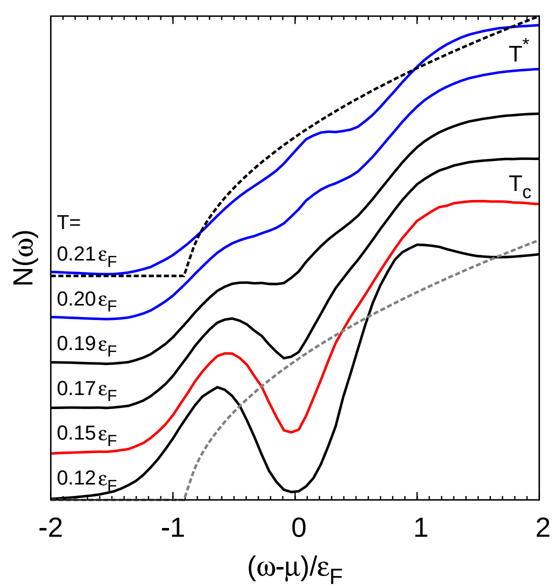

FIG. 1: (Color online) Temperature evolution of the density of states profiles, extracted from the QMC simulations [7]. The (blue) lines marked $T^* \approx 0.2\,\varepsilon_F$ correspond to the onset of the pseudogap regime, the (red) line marked $T_c = 0.15\,\varepsilon_F$ corresponds to the critical temperature. The profiles for $T = 0.21\,\varepsilon_F$ and $T = 0.12\,\varepsilon_F$ are compared with the density of states for a Fermi liquid (dashed lines).

The most striking feature of the pseudogap regime is the behavior of the fermionic density of states, which shows a dramatic depletion at the Fermi level. This was confirmed to exist in Quantum Monte Carlo (QMC) simulations of the UFG [6, 7], see Fig. 1, as well as in experiments [8–10]. The transition from a pseudogap to a normal state in the UFG is somewhat similar to a gas-plasma transition, where no discontinuities are observed, which makes it difficult to observe. Indeed, no observable imprints on the thermodynamic properties have been detected in experiments so far [11, 12], while at the same time theory also predicts none [6, 7, 13, 14]. A direct measurement of the *local* density of states of a UFG in a trap is desirable. However, one can suggest different kinds of measurements as well. A strongly paired, but not necessarily superfluid, system would respond qualitatively differently to an external probe than a non-paired system, if one were to try to separate the two fermions in a pair. In particular, in a paired system the spin susceptibility and spin conductivity should be significantly suppressed when compared to the unpaired regime. One should therefore observe a marked difference between the response of a system in the pseudogap regime from a normal Fermi liquid one, which is the expected behavior at temperatures greater than T^*.

Inspired by recent measurements of various spin responses like the spin susceptibility [15], spin transport coefficients [16] or dynamic (spin) structure factors [17], we present here an *ab initio* evaluation of the spin susceptibility χ_s and the spin conductivity σ_s for unpolarized homogeneous unitary Fermi gas. We show that both of these quantities carry a strong signal indicating survival of the Cooper pairs above the critical temperature. Our new results are consistent with previous studies [6, 7], where the existence of the pseudogap regime was found between the critical temperature $T_c = 0.15(1)\,\varepsilon_F$ and $T^* = 0.19(2)\,\varepsilon_F$, where $\varepsilon_F = p_F^2/2m$ is the free Fermi gas energy, $p_F = \hbar\,(3\pi^2 n)^{1/3}$ is the Fermi momentum corresponding to the total particle number density n. While in the previous estimation of the T^* temperature finite resolution of the method provided only the lower bound, the analysis of the spin responses allows us to provide a significantly more accurate interval for the pseudogap onset.

Moreover, the computed responses allow us to extract the temperature dependence of the spin diffusion coefficient from first principle calculations. There has been considerable speculation as to whether the transport coefficients possess universal lower bounds imposed by quantum mechanics. The best known example is a conjecture formulated by Kovtun, Son, and Starinets of the existence of a lower bound $\eta/s \geqslant \hbar/(4\pi k_B)$ on the ratio of the shear viscosity η to the entropy density s for all fluids [18]. While in our previous work [19] we found that PIMC is compatible with a well defined minimum for the η/s ratio in the vicinity of the critical temperature, here we show that the spin diffusion does not exhibit a similar minimum as a function of temperature.

To determine the spin properties of the UFG we employ the Path Integral Monte Carlo (PIMC) technique on the lattice, which provides numerically exact results, up to quantifiable systematic uncertainties (for details see Ref. [13]). Since the pseudogap regime is expected to exist in a rather small temperature region $0.15 \lesssim T/\varepsilon_F \lesssim 0.2$ it needs to be checked if it survives when the thermodynamic $V \to \infty$ and continuum $n \to 0$ limits are recovered. This step is of great importance as the critical temperature approaches the value $T_c = 0.15(1)\,\varepsilon_F$ only in the thermodynamic and continuum limits [13]. At the same time the temperature T^* above which there are no Cooper pairs left, and which reflects short range correlations among particles, does not show a similar strong volume dependence. To check the stability of the results, as the thermodynamic and continuum limit are approached, we performed simulations using three lattices $N_x = 8, 10, 12$ with corresponding average density $n \simeq 0.08, 0.04$ and 0.03, respectively. The systematic errors related to finite volume effects as well as effective-range corrections, are estimated to be likely $\sim 10-15\%$, while the statistical errors of the PIMC data are below 1%, see [20] for more details. Henceforth we define units: $\hbar = m = k_B = 1$.

The spin susceptibility as well as the spin conductivity can be theoretically determined using linear response theory via the Kubo relations. The uniform static spin susceptibility $\chi_s = \partial(n_\uparrow - n_\downarrow)/\partial(\mu_\uparrow - \mu_\downarrow)$ is obtained as [21]

$$\chi_s = \lim_{q\to 0} \frac{1}{V}\int_0^\beta d\tau \langle \hat{s}^z_{\boldsymbol{q}}(\tau)\hat{s}^z_{-\boldsymbol{q}}(0)\rangle, \tag{1}$$

where $\hat{s}^z_{\boldsymbol{q}} = \hat{n}_{\boldsymbol{q}\uparrow} - \hat{n}_{\boldsymbol{q}\downarrow}$ represents a difference between spin-selective particle number operators in Fourier representation $\hat{n}_{\boldsymbol{q}\lambda} = \sum_{\boldsymbol{p}} \hat{a}^\dagger_\lambda(\boldsymbol{p})\,\hat{a}_\lambda(\boldsymbol{p}+\boldsymbol{q})$, $\beta = 1/T$ is the inverse temperature and $\langle \ldots \rangle$ stands for the grand-canonical ensemble average. The imaginary-time dependence of an operator is generated as $\hat{O}(\tau) = e^{\tau(\hat{H}-\mu\hat{N})}\hat{O}e^{-\tau(\hat{H}-\mu\hat{N})}$, where $\hat{H}$ is the Hamiltonian of the system, μ is the chemical potential, and $\hat{N}$ is the particle number operator. The expectation values can be evaluated directly for $q = 0$. In this case the spin operator $\hat{s}^z_{\boldsymbol{q}=0}$ commutes with the Hamiltonian and the expectation value is τ-independent. Consequently, the QMC calculation consists in the evaluation of the expectation value of a two-body operator, and the static spin susceptibility can be computed very accurately within our framework.

In Fig. 2, the static spin susceptibility χ_s in units of free Fermi gas susceptibility $\chi_0 = 3n/2\varepsilon_F$ is shown for temperature range $0.1 \leqslant T/\varepsilon_F \leqslant 0.5$. The results on 8^3, 10^3 and 12^3 lattices exhibit satisfactory agreement with each other and no systematic trend in the data has

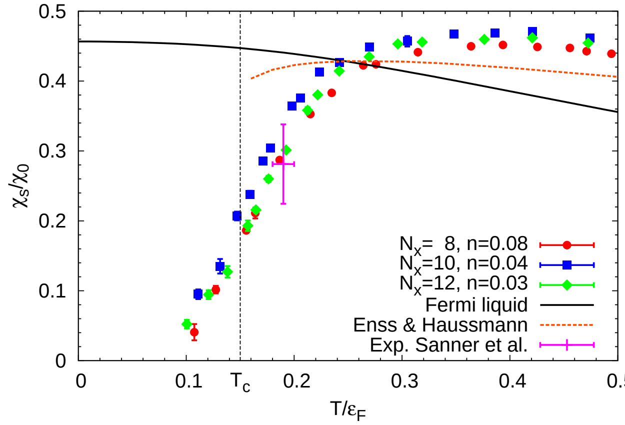

FIG. 2: (Color online) The static spin susceptibility as a function of temperature for an 8^3 lattice solid (red) circles, 10^3 lattice (blue) squares and 12^3 lattice (green) diamonds. Vertical black dotted line indicates the critical temperature of superfluid to normal phase transition $T_c = 0.15\,\varepsilon_F$. For comparison Fermi liquid theory prediction and recent results of the T-matrix theory produced by Enss and Haussmann [25] are plotted with solid and dashed (brown) lines, respectively. The experimental data point from Ref. [15] is also shown.

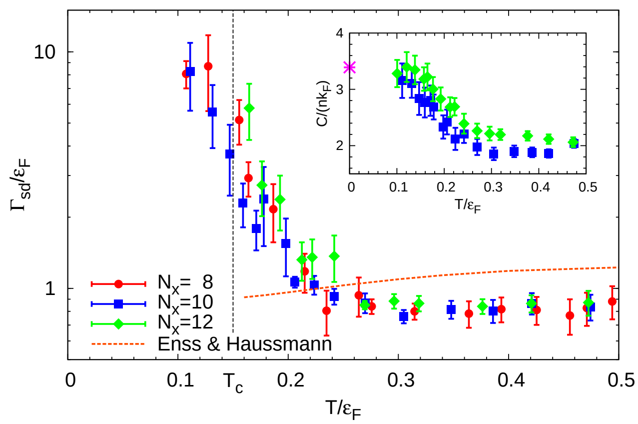

FIG. 3: (Color online) The spin drag rate $\Gamma_{sd} = n/\sigma_s$ in units of Fermi energy as a function of temperature for an 8^3 lattice solid (red) circles, 10^3 lattice (blue) squares and 12^3 lattice (green) diamonds. Vertical black dotted line locates the critical temperature of superfluid to normal phase transition. Results of the T-matrix theory are plotted by dashed (brown) line [25]. The inset shows extracted value of the contact density as function of the temperature. The (purple) asterisk shows the contact density from the QMC calculations of Ref. [29] at $T = 0$.

been detected as we approach the thermodynamic and the continuum limit. For temperatures $0.25\,\varepsilon_F - 0.5\,\varepsilon_F$ no strong temperature dependence of the spin susceptibility is observed. The latter is well below the susceptibility of the free Fermi gas with a value around $\chi_s \approx 0.45\,\chi_0$, which is in qualitative agreement with the Fermi liquid picture as well as results of other groups [22–26]. In the interval $T^* = 0.20 - 0.25\,\varepsilon_F$ we find beginning of pronounced suppression of the spin susceptibility, which we associate with the existence of Cooper pairs in the system. Note that already at T_c the spin susceptibility is about half its value at the onset of suppression (roughly $T = 0.25\,\varepsilon_F$). Thus, two temperature scales are clearly distinguishable: the critical temperature of superfluid-to-normal phase transition $T_c = 0.15\,\varepsilon_F$, and the onset of the Cooper-pair formation T^*.

The static spin conductivity σ_s represents another quantity which is expected to be strongly affected by the presence of the Cooper pairs as it measures response of the spin current $\boldsymbol{j}_s = \boldsymbol{j}_\uparrow - \boldsymbol{j}_\downarrow$ once the weak external $\boldsymbol{F}$ force which couples with opposite signs to the two spin populations is applied to the system, i.e. $\boldsymbol{j}_s = \sigma_s \boldsymbol{F}$. In order to extract the spin conductivity we consider the Kubo formula, which relates the frequency-dependent spin conductivity to the corresponding spectral density: $\sigma_s(\omega) = \pi\rho_s^{(jj)}(\boldsymbol{q} = 0, \omega)/\omega$; while the static spin conductivity is defined in the limit of zero frequency: $\sigma_s = \lim_{\omega\to 0^+} \sigma_s(\omega)$. The spectral density $\rho_s^{(jj)}(\boldsymbol{q}, \omega)$ is related to the imaginary-time (Euclidean) current-current correlator provided by the PIMC method

$$G_s^{(jj)}(\boldsymbol{q}, \tau) = \frac{1}{V}\langle[\hat{j}^z_{\boldsymbol{q}\uparrow}(\tau) - \hat{j}^z_{\boldsymbol{q}\downarrow}(\tau)][\hat{j}^z_{-\boldsymbol{q}\uparrow}(0) - \hat{j}^z_{-\boldsymbol{q}\downarrow}(0)]\rangle, \tag{2}$$

by inversion of the spectral relation

$$G_s^{(jj)}(\boldsymbol{q}, \tau) = \int_0^\infty \rho_s^{(jj)}(\boldsymbol{q}, \omega)\,\frac{\cosh\left[\omega(\tau - \beta/2)\right]}{\sinh\left(\omega\beta/2\right)}\,d\omega, \tag{3}$$

where $\hat{j}^z_{\boldsymbol{q}\lambda}(\tau)$ stands for the third component of Fourier representation of the spin-selective current operator. To invert Eq. (3) we have applied the methodology which combines two complementary methods: singular value decomposition (SVD) and maximum entropy method (MEM), both described in Ref. [27]. An additional *a priori* information include the non-negativity of the spin conductivity $\sigma_s(\omega) \geqslant 0$, a Lorentzian-like structure at low frequencies (Drude model) and the asymptotic tail behavior $\sigma_s(\omega\to\infty) = C/(3\pi\omega^{3/2})$, where C is Tan contact density [25]. The contact density was extracted from the tail of the momentum distribution $n(p) \sim Cp^{-4}$, using a technique similar to that of Ref. [28]. As the universal decay of the tail distribution starts around $p/p_F \approx 2$, we were unable to extract the contact for the $N_x = 8$ lattice. In that case we used the value of C extracted from the $N_x = 10$ lattice. The inset of Fig. 3 shows the temperature dependence of the contact density used as *a priori* information. For calculations in the $N_x = 12$ lattice, we found that the signal-to-noise ratio for the correlators at $T < 0.16\,\varepsilon_F$ is insufficient to perform a

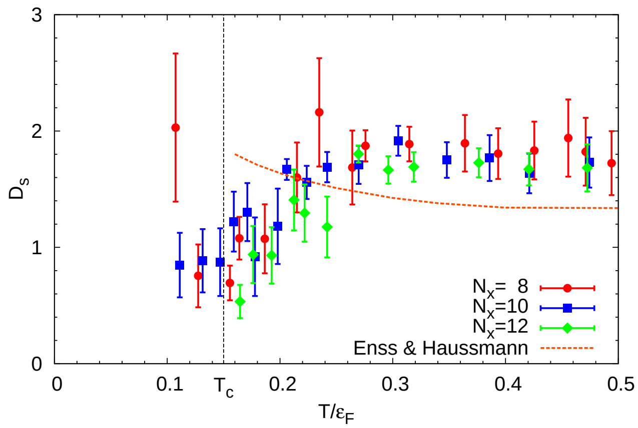

FIG. 4: (Color online) The spin diffusion coefficient obtained by the Einstein relation $D_s = \sigma_s/\chi_s$ as function of temperature. The notation is identical to Fig. 3.

stable reconstruction of the spectral density. For more details about the reconstruction process see [20].

In Fig. 3 we present the inverse of the static spin conductivity called the spin drag rate $\Gamma_{sd} = n/\sigma_s$, which is the rate of the momentum transfer between fermions with opposite spins. For $T = 0.25\,\varepsilon_F - 0.5\,\varepsilon_F$, no strong temperature dependence is observed. For all three lattices the spin drag rate exhibits a significant enhancement above T_c, in the interval $T^* = 0.20-0.25\,\varepsilon_F$, which is consistent with the occurrence of the spin susceptibility suppression. Such an enhancement is expected for a system with strong correlations between particles of opposite spins.

Finally, the computed spin susceptibility and spin conductivity allow us to extract the spin diffusion coefficient D_s in a fully *ab initio* manner. In the hydrodynamic regime it defines the proportionality between the spin current $\boldsymbol{j}_s$ and spatially varying polarization by Fick's law $\boldsymbol{j}_s = -D_s\boldsymbol{\nabla}(n_\uparrow - n_\downarrow)$. The spin diffusivity D_s can be related to the spin conductivity and the spin susceptibility by the Einstein relation $D_s = \sigma_s/\chi_s$. In Fig. 4 we show the temperature evolution of the spin diffusion coefficient. In the normal phase, for temperatures $0.25\,\varepsilon_F - 0.5\,\varepsilon_F$ the diffusivity is approximately constant $D_s \approx 1.8$. Surprisingly, we find that the spin diffusion coefficient decreases substantially when the system enters the pseudogap regime, acquiring eventually a value around $D_s \approx 0.8$ in the superfluid phase. Such a low value can be understood as a quantum limit for this transport coefficient. The bound originates from kinetic theory, where $D_s \sim vl$, v is the average particle speed, and l is the mean free path. For a strongly correlated system, the product of $v \sim p_F \sim n^{1/3}$ and $l \sim n^{-1/3}$ cancels the density dependence, giving $D_s \sim 1$.

In Ref. [30] the existence of a minimal value of the diffusivity was predicted for a temperature somewhat below the Fermi temperature, within Landau-Boltzmann theory. Recently, it was reported that Luttinger-Ward theory sets the minimum $D_s \simeq 1.3$ at $T = 0.5\,\varepsilon_F$ [25]. Our *ab initio* calculations do not confirm the presence of a minimum for the spin diffusion coefficient down to $T = 0.1\,\varepsilon_F$, and they do not rule out possibility that the diffusivity D_s decreases further when temperature is lowered.

Our results for the spin susceptibility and the spin drag rate deviate from the recent measurements of MIT group [16] extracted from fully polarized cloud collisions. This technique, in which two noninteracting clouds collide, and in which pairs do not exist and likely are not formed, is less suitable to probe the low temperature regime, where pairs already exist and their presence is of crucial importance. Pair formation in such an experiment would require three-body collisions. Recent theoretical simulations [23, 31, 32] demonstrated that this experiment can be explained assuming that the measurement explores a non-equilibrium state associated with a quasi-repulsive Fermi gas and two-body collisions alone. On the other hand, the technique based on speckle imaging of spin fluctuations, used to measure the spin susceptibility of the system in thermal equilibrium [15], is in remarkable agreement with our theoretical results, see Fig. 2.

In summary, we have presented results for the spin response of the UFG at finite temperature, obtained through an *ab initio* PIMC approach. The spin susceptibility and the spin conductivity bear signatures of Copper-pair formation above the critical temperature $T_c \simeq 0.15\,\varepsilon_F$ up to $T^* \approx 0.20-0.25\,\varepsilon_F$. The spin diffusion coefficient does not display a minimum in the vicinity of the critical temperature, but instead drops to very low values $D_s \approx 0.8$ in the superfluid phase. We showed that the spin response of a unitary Fermi gas is not affected by the superfluid to normal transition, but only by the presence of Cooper pairs, and all these spin observables show a smooth and monotonic behavior up to the temperature T^*, where the pseudogap cease to show up in the density of states.

We thank T. Enss for providing us with the T-matrix results [25]. We acknowledge support under U.S. DOE Grant Nos. DE-FG02-97ER41014 and DE-FC02-07ER41457, and Contract No. N N202 128439 of the Polish Ministry of Science. One of the authors (G.W.) acknowledges the Polish Ministry of Science for the support within the program "Mobility Plus-I edition" under Contract No. 628/MOB/2011/0. Calculations reported here have been, performed at the Interdisciplinary Centre for Mathematical and Computational Modelling (ICM) at Warsaw University and on the University of Washington Hyak cluster funded by the NSF MRI Grant No. PHY-0922770.

Note added. Similar studies of $\chi_s(T)$ and density of states in an attractive 2D Hubbard model (in the context of cuprates) have been performed in Refs. [33]. There are however qualitative differences between the physics of the attractive 2D Hubbard model and dilute Fermi gases in 2D, which are practically non-interacting, see chapter 7 in Ref. [2].

[1] S Giorgini, L.P. Pitaevskii, and S. Stringari, Rev. Mod. Phys. **80**, 1215 (2008); I. Bloch, J. Dalibard, and W. Zwerger, Rev. Mod. Phys. **80**, 885 (2008).

[2] *The BCS-BEC crossover and the unitary Fermi Gas* Lecture Notes in Physics, edited by W. Zwerger (Springer-Verlag, Berlin, 2012), Vol. 836.

[3] A. Perali, P. Pieri, G. C. Strinati, and C. Castellani, Phys. Rev. B **66**, 024510 (2002).

[4] Q. Chen, J. Stajic, S. Tan, and K. Levin, Phys. Rep. **412**, 1 (2005).

[5] N. Iwamoto and C.J. Pethick, Phys. Rev. D **25**, 313 (1982); G. Shen, S. Gandolfi, S. Reddy, and J. Carlson, arXiv:1205.6499.

[6] P. Magierski, G. Wlazłowski, A. Bulgac, and J.E. Drut, Phys. Rev. Lett. **103**, 210403 (2009).

[7] P. Magierski, G. Wlazłowski, and A. Bulgac, Phys. Rev. Lett. **107**, 145304 (2011).

[8] J.T. Stewart, J.P. Gaebler, and D.S. Jin, Nature **454**, 744 (2010).

[9] J.P. Gaebler, *et al.,* Nature Physics **6**, 569 (2010).

[10] A. Perali, *et al.,* Phys. Rev. Lett. **106**, 060402 (2011).

[11] S. Nascimbéne, *et al.,* Phys. Rev. Lett. **106**, 215303 (2011).

[12] M. J. H. Ku, A. T. Sommer, L. W. Cheuk, and M. W. Zwierlein, Science **335**, 563 (2012).

[13] A. Bulgac, J.E. Drut, and P. Magierski, Phys. Rev. A **78** 023625 (2008).

[14] J.E. Drut, T.A. Lahde, G. Wlazlowski, and P. Magierski, Phys. Rev. A **85**, 051601(R) (2012).

[15] C. Sanner, *et al.,* , Phys. Rev. Lett **106**, 010402 (2011).

[16] A. Sommer, M. Ku, G. Roati, and M. W. Zwierlein, Nature **472**, 201 (2011).

[17] S. Hoinka, M. Lingham, M. Delehaye, and C. J. Vale, Phys. Rev. Lett. **109**, 050403 (2012).

[18] P.K. Kovtun, D.T. Son, and A.O. Starinets, Phys. Rev. Lett. **94**, 111601 (2005).

[19] G. Wlazłowski, P. Magierski, and J.E. Drut, Phys. Rev. Lett. **109**, 020406 (2012).

[20] See Supplemental Material for discussion of the systematic errors and technical details concerning the inversion procedure.

[21] G. D. Mahan, *Many-particle physics*, New York (2000).

[22] D. Wulin, H. Guo, C.-C. Chien, and K. Levin, Phys. Rev. A **83**, 061601(R) (2011).

[23] F. Palestini, P. Pieri, and G. C. Strinati, Phys. Rev. Lett. **108**, 080401 (2012).

[24] T. Kashimura, R. Watanabe, and Y. Ohashi, Phys. Rev. A **86**, 043622 (2012).

[25] T. Enss and R. Haussmann, Phys. Rev. Lett. **109**, 195303 (2012).

[26] M. P. Mink, *et al.,* Phys. Rev. A **86**, 063631 (2012).

[27] P. Magierski and G. Wlazłowski, Comput. Phys. Commun. **183**, 2264 (2012).

[28] J.E. Drut, T.A. Lähde, and T. Ten, Phys. Rev. Lett. **106**, 205302 (2011).

[29] S. Hoinka, *et al.,* arXiv:1209.3830.

[30] G. M. Bruun, New J. Phys. **13**, 035005 (2011).

[31] E. Taylor, S. Zhang, W. Schneider, and M. Randeria, Phys. Rev. A **84**, 063622 (2011).

[32] O. Goulko, F. Chevy, and C. Lobo, Phys. Rev. A **84**, 051605 (2011).

[33] M. Randeria, N. Trivedi, A. Moreo, and R.T. Scalettar, Phys. Rev. Lett. **69**, 2001 (1992); N. Trivedi and M. Randeria, Phys. Rev. Lett. **75**, 312 (1995).